JOURNAL OF AIRCRAFT
Vol. 39, No. 2, March–April 2002

Aeroelastic Divergence of Stiffened Composite Multicell Wing Structures

Chyanbin Hwu* and Z. S. Tsai†
National Cheng-Kung University, Tainan 70101, Taiwan, Republic of China

When the wing is treated as a composite sandwich plate and it is assumed that the wing chordwise section is rigid, mathematical formulations for the stiffened composite multicell wing structures are provided, and associated governing equations for the aeroelastic divergence are also derived by a direct approach. When the matrix notation is used, the system of equations is written into an explicit and simple mathematical expression that can then be solved explicitly by using the technique of Laplace integral transform. In this modeling, the composite wing skins and stringers (including the spar flanges) are simulated as the faces, whereas the spar webs and ribs are simulated as the core of the sandwiches. Because the wing cross section must have a streamline shape, unlike the usual uniform thickness modeling, it is more appropriate to simulate the wings as variable thickness sandwiches where the thickness is a function of the airfoil. Moreover, as is usual for assumptions for the sandwich plates, the effects of the transverse shear deformation are also considered. Because several special conditions have been studied in the literature, we first compare our solutions with some existing solutions. To show the generality, several illustrative examples are given to consider the effects of spars, skins (including the ply orientation and stacking sequence), stringers, swept angles, aspect ratio, shape of airfoil, and the warping restraints on the divergence dynamic pressures and the lift loads redistribution.

Introduction

THE fundamental work concerning the divergence instability of swept metallic wings was done about 50 years ago.[1] It was shown that bending deflections have a destabilizing effect on the sweptforward wings. Hence, the sweptforward wing aircraft as a possible option was completely eliminated for a long time, until the aeroelastic tailoring concept for the composite wing structures was raised and studied by Krone.[2] Following his work, many different approaches and considerations have been studied, such as the works done by Lerner and Markowitz,[3] Weisshaar,[4] Oyibo,[5] Lottati,[6] and a series work done by Librescu and Simovich,[7] Librescu and Khdeir,[8] Librescu and Thangjitham,[9] and Karpouzian and Librescu.[10] They first considered the warping restraint effects,[7–9] then considered the effects of transverse shear strains.[10] All of these results support that a composite sweptforward wing can be tailored to overcome this adverse instability phenomenon.

Most of the governing equations provided in the literature are obtained from Hamilton's variational principle. Because of the complexity of the formulation, it is difficult to see any physical indication purely from the complicated mathematical equations. Hence, it is not easy to extend the formulation to more realistic wing structures such as stiffened multicell wings that are composed of the skins, stringers, ribs, and spars. In this paper, a direct approach using the equilibrium equations for the composite sandwich plates proposed by Hwu and Hu[11] and Hu and Hwu[12] was employed to formulate the problems. The final mathematical formulation turns out to be a rather simple equation and can be proved to be equivalent to those derived in the literature. Because of its simplicity, the physical meaning of each equation is clear and, hence, is easy to be used to consider more complicated structures such as nonuniform stiffened composite multicell wings discussed in this paper. Moreover, the important factors, such as the warping restraint, transverse shear strain, shape of airfoil, aspect ratio, swept angle, fiber orientation, ply stacking sequence, stringers, and spars, are all included in our formulation without adding too much complexity. The solving of the aeroelastic divergence is then performed by the equation written in an explicit matrix form.

Received 19 July 2000; revision received 19 July 2001; accepted for publication 26 July 2001.

*Professor, Institute of Aeronautics and Astronautics.
†Graduate Student, Institute of Aeronautics and Astronautics.

Formulation of Composite Sandwich Plates

The primary function of the wing structure is providing the lift for an aircraft, which is governed by the aerodynamic consideration. In addition to the aerodynamic pressure, there are other forces resisted by the wing structures such as the weight of the structures, fuels, engines, undercarriage system, and/or possible carried weapons, the thrust of engines, etc. To sustain these loads, the wing structures are usually designed as that shown in Fig. 1, which consists of axial members in stringers, bending members in spars, shear panels in the cover skin and spar webs, and planar members in ribs. If the cover skin of the wing is made of the composite laminates, the entire wing structure may be simulated by a composite sandwich plate in which the wing skins and stringers (including the spar flanges) are simulated as the faces, whereas the spar webs and ribs are simulated as the core of the sandwiches. Because the wing cross section must have a streamline shape commonly referred to as an airfoil section, the thickness of the sandwich will not be a constant but a function of the airfoil. Moreover, as the usual sandwich assumptions, the thickness is not too small to neglect the transverse shear deformation. Based on these considerations, a mathematical model for the composite sandwich plates proposed by Hwu and Hu[11] will be applied in this paper. For completeness, and for the convenience of the readers, we now list the basic equations for the composite sandwich plates.

Displacement Fields

Like the Euler's beam theory, the classical plate theory is derived based on Kirchhoff's hypotheses[13] that the transverse shear deformation is negligible. The generalization of the classical plate theory with respect to the effect of transverse shear deformation is substantially due to Reissner.[14] In this theory, the displacement field u, v, and w is assumed to be a linear function of z, where z is the coordinate in the thickness direction, that is,

$$u = u_0 + z\beta_x, \qquad v = v_0 + z\beta_y, \qquad w = w_0 \tag{1}$$

where u_0, v_0, and w_0 are the midplane displacements in the x, y, and z directions, and β_x and β_y are the rotation angles with respect to

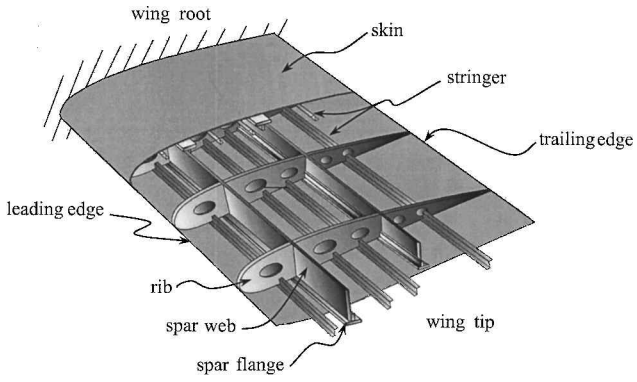

Fig. 1 Composite wing structure arrangements.

x and y axes, respectively. Moreover, u_0, v_0, w_0, β_x, and β_y are all functions of x and y only. The rotation angles β_x and β_y are related to the transverse shear strains γ_{xz} and γ_{yz} by

$$\beta_x = \gamma_{xz} - \frac{\partial w}{\partial x} \tag{2a}$$

$$\beta_y = \gamma_{yz} - \frac{\partial w}{\partial y} \tag{2b}$$

Strain–Displacement Relations

From the displacement fields assumed in Eq. (1), and the small strain definitions, the strains ε_x, ε_y, and γ_{xy} of the sandwich plates may be expressed in terms of the midplane strains ε_{x0}, ε_{y0}, and γ_{xy0} and the curvature κ_x, κ_y, and κ_{xy} as follows:

$$\varepsilon_x = \varepsilon_{x0} + z\kappa_x, \qquad \varepsilon_y = \varepsilon_{y0} + z\kappa_y, \qquad \gamma_{xy} = \gamma_{xy0} + z\kappa_{xy} \tag{3a}$$

where

$$\varepsilon_{x0} = \frac{\partial u_0}{\partial x}, \qquad \varepsilon_{y0} = \frac{\partial v_0}{\partial y}, \qquad \gamma_{xy0} = \frac{\partial u_0}{\partial y} + \frac{\partial v_0}{\partial x} \tag{3b}$$

$$\kappa_x = \frac{\partial \beta_x}{\partial x}, \qquad \kappa_y = \frac{\partial \beta_y}{\partial y}, \qquad \kappa_{xy} = \frac{\partial \beta_x}{\partial y} + \frac{\partial \beta_y}{\partial x} \tag{3c}$$

Stress–Strain Relations

Because the dimension of the thickness is relatively smaller than that of the plane direction, it is hoped that the plate problems can be formulated in terms of the functions varying with respect to x and y only. Equation (3) shows that the strain field can be expressed in terms of the midplane strains and curvatures, which are functions of x and y only. For the stresses, the two-dimensional representatives are best presented by the stress resultants N_x, N_y, N_{xy}, Q_x, and Q_y and the bending moments M_x, M_y, and M_{xy} defined as

$$\begin{Bmatrix} N_x \\ N_y \\ N_{xy} \end{Bmatrix} = \sum_{k=1}^{n} \int_{z_{k-1}}^{z_k} \begin{Bmatrix} \sigma_x \\ \sigma_y \\ \tau_{xy} \end{Bmatrix}_k \mathrm{d}z$$

$$\begin{Bmatrix} M_x \\ M_y \\ M_{xy} \end{Bmatrix} = \sum_{k=1}^{n} \int_{z_{k-1}}^{z_k} \begin{Bmatrix} \sigma_x \\ \sigma_y \\ \tau_{xy} \end{Bmatrix}_k z\,\mathrm{d}z$$

$$\begin{Bmatrix} Q_x \\ Q_y \end{Bmatrix} = \sum_{k=1}^{n} \int_{z_{k-1}}^{z_k} \begin{Bmatrix} \tau_{xz} \\ \tau_{yz} \end{Bmatrix}_k \mathrm{d}z \tag{4}$$

where the laminas number n includes all of the lamina on the upper and lower faces and z_k and z_{k-1} are defined in Fig. 2. For the sandwich construction, the in-plane stress resultants N_x, N_y, and N_{xy} and bending moments M_x, M_y, and M_{xy} are almost contributed by

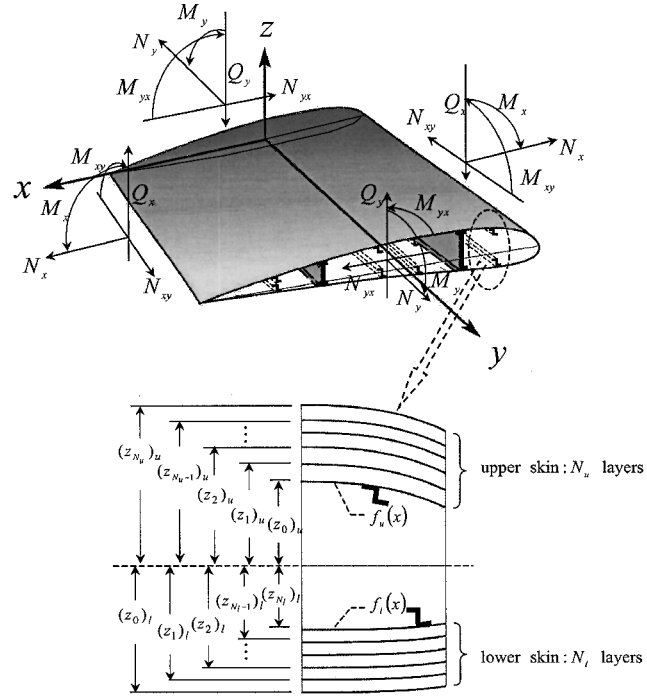

Fig. 2 Sign convention of the composite sandwich plates.

the faces, whereas the transverse shear forces Q_x and Q_y are undertaken by the core. Similar to the classical lamination theory,[15] the relation between the stress resultants and midplane strains and curvatures are

$$\begin{Bmatrix} N_x \\ N_y \\ N_{xy} \\ M_x \\ M_y \\ M_{xy} \end{Bmatrix} = \begin{bmatrix} A_{11} & A_{12} & A_{16} & B_{11} & B_{12} & B_{16} \\ A_{12} & A_{22} & A_{26} & B_{12} & B_{22} & B_{26} \\ A_{16} & A_{26} & A_{66} & B_{16} & B_{26} & B_{66} \\ B_{11} & B_{12} & B_{16} & D_{11} & D_{12} & D_{16} \\ B_{12} & B_{22} & B_{26} & D_{12} & D_{22} & D_{26} \\ B_{16} & B_{26} & B_{66} & D_{16} & D_{26} & D_{66} \end{bmatrix} \begin{Bmatrix} \varepsilon_{x0} \\ \varepsilon_{y0} \\ \gamma_{xy0} \\ \kappa_x \\ \kappa_y \\ \kappa_{xy} \end{Bmatrix} \tag{5a}$$

$$\begin{Bmatrix} Q_x \\ Q_y \end{Bmatrix} = \begin{Bmatrix} A_{55}\gamma_{xz} \\ A_{44}\gamma_{yz} \end{Bmatrix}, \qquad A_{55} = khG_{xz}, \qquad A_{44} = khG_{yz} \tag{5b}$$

where h is the thickness of the core and may be a function of x, G_{xz} and G_{yz} are transverse shear moduli in x–z and y–z planes, and k is the transverse shear correction factor and is selected to be $\frac{5}{6}$ for the present paper.[16] A_{ij}, B_{ij}, and D_{ij}, $i, j = 1, 2, 6$, are, respectively, the extensional, coupling, and bending stiffnesses, which are related to the location z_k and the transformed reduced stiffnesses $\bar{Q}_{ij}$ of each lamina as

$$A_{ij} = \sum_{k=1}^{n} (\bar{Q}_{ij})_k (z_k - z_{k-1}), \qquad B_{ij} = \frac{1}{2} \sum_{k=1}^{n} (\bar{Q}_{ij})_k \left(z_k^2 - z_{k-1}^2\right)$$

$$D_{ij} = \frac{1}{3} \sum_{k=1}^{n} (\bar{Q}_{ij})_k \left(z_k^3 - z_{k-1}^3\right), \qquad i, j = 1, 2, 6 \tag{6}$$

Unlike the classical lamination theory in which A_{ij}, B_{ij}, and D_{ij} are calculated based on the coordinate where $z = 0$ is the middle surface of the laminate, here the plane $z = 0$ is located on the midsurface of the sandwiches.

Equilibrium Equations

The equilibrium equations expressed in terms of the stress resultants and bending moments are

$$\sum F_x = 0 : \frac{\partial N_x}{\partial x} + \frac{\partial N_{xy}}{\partial y} + p_x = 0$$

$$\sum F_y = 0 : \frac{\partial N_{xy}}{\partial x} + \frac{\partial N_y}{\partial y} + p_y = 0$$

$$\sum F_z = 0 : \frac{\partial Q_x}{\partial x} + \frac{\partial Q_y}{\partial y} + p = 0$$

$$\sum M_x = 0 : \frac{\partial M_x}{\partial x} + \frac{\partial M_{xy}}{\partial y} + m_x = Q_x$$

$$\sum M_y = 0 : \frac{\partial M_{xy}}{\partial x} + \frac{\partial M_y}{\partial y} + m_y = Q_y \qquad (7)$$

where p_x, p_y, p, and m_x and m_y are the total distributed loads and moments applied on the upper and lower surfaces of the sandwich plates.

Boundary Conditions

When Eqs. (3) and (5) are used, the five equilibrium equations for the composite sandwich plates given in Eq. (7) can be written in terms of five unknowns u_0, v_0, w_0, β_x, and β_y. Theoretically, the solutions can be found by solving these five coupled partial differential equations with the proper boundary conditions. In applications, several different boundary conditions may occur. Generally, they can be classified as geometrical, static, and mixed boundary conditions. Regardless of kind of boundary conditions, they all can be expressed as

$$k_{ui}(u_i - \bar{u}_i) = k_{Ni}(N_i - \bar{N}_i), \qquad i = 1, 2, 3, 4, 5 \qquad (8)$$

where $u_i, i = 1, 2, 3, 4, 5$, include the midplane displacements u_n, u_t, and w_0 and the rotation angles β_n and β_t. Here N_i are the corresponding force terms N_n, N_{nt}, Q_n, M_n, and M_{nt}. The subscripts n and t represent the directions of the normal and tangent of the boundary, respectively. The overbar means the prescribed values at the boundaries. Except for the category of elastic support and restraint, generally either k_{ui} or k_{Ni}, $i = 1, 2, 3, 4, 5$, are equal to zero. For the geometrical boundary condition, all $k_{Ni} = 0$, whereas for the static boundary condition, all $k_{ui} = 0$. As to the mixed boundary condition, only parts of k_{ui} and k_{Ni} are equal to zero. In the case of a rectangular sandwich plate with edges parallel to the x and y axes, the geometrical, static, or mixed boundary conditions along $y = \text{const}$ can generally be expressed as

$$N_{xy} = \bar{N}_{xy}, \quad \text{or} \quad u_0 = \bar{u}_0$$

$$N_y = \bar{N}_y, \quad \text{or} \quad v_0 = \bar{v}_0$$

$$Q_y = \bar{Q}_y, \quad \text{or} \quad w_0 = \bar{w}_0$$

$$M_{xy} = \bar{M}_{xy}, \quad \text{or} \quad \beta_x = \bar{\beta}_x$$

$$M_y = \bar{M}_y, \quad \text{or} \quad \beta_y = \bar{\beta}_y \qquad (9)$$

When the plate is thin, it is usually assumed that the transverse shear deformation can be neglected, that is, $\gamma_{xz} = \gamma_{yz} = 0$. Substituting this assumption into Eq. (2), we obtain $\beta_x = -w_{,x}$ and $\beta_y = -w_{,y}$. This means that the rotation angles β_x and β_y are dependent on the deflection w only. By this assumption, the equations associated with the bending moment equilibrium should be combined into the vertical force equilibrium, and the boundary conditions associated with vertical displacements (or forces) and the rotation angles (or bending moments) should also be modified.

Modeling of Stiffened Composite Multicell Wing Structures

Because of the closely spaced stringers and the transverse stiffening members like wing spars and ribs, in aircraft analysis it is usually assumed that the wing chordwise section is rigid.[17] Moreover, by treating wing skins, stringers, and the spar flanges as the sandwich faces, and wing spar webs and ribs as the sandwich cores, the stiffened composite multicell wing structures may also be modeled as a composite sandwich plate.

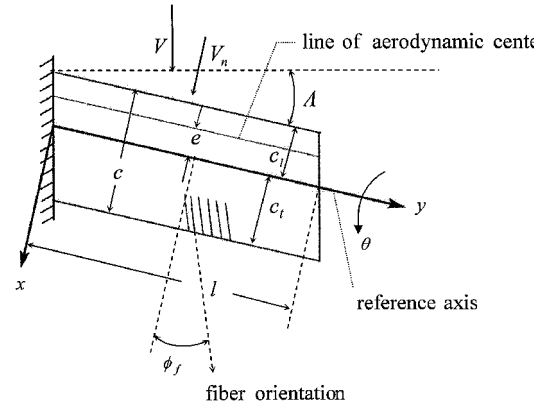

Fig. 3 Geometry of the composite cantilever swept wings.

Rigid-Wing Chordwise Section

Consistent with the chordwise-rigid postulation, the midplane displacement and rotation angles shown in Eq. (1) may be assumed to be

$$u_0 = 0 \qquad (10a)$$

$$v_0 = v_0(y) \qquad (10b)$$

$$w_0 = w_f(y) - x\theta(y) \qquad (10c)$$

$$\beta_x = \theta(y) \qquad (10d)$$

$$\beta_y = \beta_f(y) + x\beta_r(y) \qquad (10e)$$

where $w_f(y)$ is the deflection (positive upward) measured at the line of the flexural center, which is now selected as the reference axis shown in Fig. 3, and $\theta(y)$ is the twist around the flexural axis (positive nose up). The relation between β_x and θ is due to the chordwise-rigid assumption, which leads to $\gamma_{xz} = 0$. By use of Eqs. (2a) and (10c) we can get Eq. (10d). However, in the spanwise direction the transverse shear deformation cannot be neglected for the thick plates. Hence, two extra functions, β_f and β_r, are needed for the representation of β_y, where β_f is the rotation angle measured at the flexural axis and β_r is the rate of angle change in the x direction. By the assumption given in Eq. (10), the midplane strains and curvatures defined in Eqs. (3b) and (3c) become

$$\varepsilon_{x0} = 0 \qquad (11a)$$

$$\varepsilon_{y0} = v_0' \qquad (11b)$$

$$\gamma_{xy0} = 0 \qquad (11c)$$

$$\kappa_x = 0 \qquad (11d)$$

$$\kappa_y = \beta_f' + x\beta_r' \qquad (11e)$$

$$\kappa_{xy} = \theta' + \beta_r \qquad (11f)$$

Modeling of Wing Skins, Stringers, and Spar Flanges

In wing structure design, most of the bending and axial loads are resisted by the stringers and spar flanges, whereas the wing skins resist almost all of the in-plane shear forces. Hence, it is reasonable to model the wing skins, stringers, and spar flanges as the sandwich faces. If the stringers and spar flanges are considered to be the fibers of a pseudolamina, by the rule of mixture[15] the equivalent material properties of this pseudolamina may be written as

$$E_L = E_s(A_s/A_p) + E_f(A_f/A_p)$$

$$v_{LT} = v_s(A_s/A_p) + v_f(A_f/A_p), \qquad E_T = 0, \qquad G_{LT} = 0 \qquad (12)$$

where E, v, G, and A are Young's modulus, Poisson's ratio, shear modulus, and cross-sectional area, respectively. The subscripts L, T, s and f denote the longitudinal direction, transverse direction, stringer, and spar flange, respectively. A_p stands for the cross-section area of pseudolamina. By adding this pseudolamina to the laminated composite skin, the face properties may be represented by A_{ij}, B_{ij}, and D_{ij} shown in Eq. (6). Note that due to the shape of the airfoil, z_k in Eq. (6) is a function of x. If the upper and lower surfaces of the airfoil are represented by $f_u(x)$ and $f_l(x)$ (Fig. 2), the stiffness matrices A_{ij}, B_{ij}, and D_{ij} of the wings are related to those of the corresponding laminated composite flat plate by

$$A_{ij}(x) = A_{ij}^F, \qquad B_{ij}(x) = B_{ij}^F + f_u(x)A_{ij}^u + f_l(x)A_{ij}^l$$

$$D_{ij}(x) = D_{ij}^F + 2f_u(x)B_{ij}^u + 2f_l(x)B_{ij}^l + f_u^2(x)A_{ij}^u + f_l^2(x)A_{ij}^l \qquad i, j = 1, 2, 6 \quad (13)$$

where, superscript F denotes the properties associated with the flat composite plates and superscripts u and l denote those of the upper and lower parts of the flat plate.

Because of the assumption given in Eq. (10), it is desirable to reduce the two-dimensional formulation given for the composite sandwich plates to an equivalent one-dimensional formulation. With this consideration, we like to integrate the stress resultants and bending moments given in Eq. (5a) with respect to x. Their relations with the midplane strains and curvatures may then be written as

$$\begin{Bmatrix} \tilde{N}_y \\ \tilde{M}_y \\ \tilde{M}_{xy} \end{Bmatrix} = \begin{bmatrix} \tilde{A}_{22} & \tilde{B}_{22} & \tilde{B}_{22}^* & \tilde{B}_{26} \\ \tilde{B}_{22} & \tilde{D}_{22} & \tilde{D}_{22}^* & \tilde{D}_{26} \\ \tilde{B}_{26} & \tilde{D}_{26} & \tilde{D}_{26}^* & \tilde{D}_{66} \end{bmatrix} \begin{Bmatrix} v_0' \\ \beta_f' \\ \beta_r' \\ \theta' + \beta_r \end{Bmatrix} \quad (14)$$

where the tilde $\sim$ denotes integration with respect to x, the superscript * multiplication by x, and the prime $'$ differentiation with respect to y. For example,

$$\tilde{D}_{22} = \int_{-c_l}^{c_t} D_{22}\,\mathrm{d}x, \qquad \tilde{D}_{22}^* = \int_{-c_l}^{c_t} D_{22}x\,\mathrm{d}x$$

$$\tilde{D}_{22}^{**} = \int_{-c_l}^{c_t} D_{22}x^2\,\mathrm{d}x, \qquad v_0' = \frac{\mathrm{d}v_0}{\mathrm{d}y}, \ldots \quad (15)$$

The lower and upper limits $-c_l$ and c_t are the location of leading and trailing edges, respectively (Fig. 3). The relations for the N_x, N_{xy}, and M_x are not shown because they play no role in a one-dimensional representation.

Modeling of Spar Webs and Ribs for Multicell Wings

A multicell wing is made by proper arrangement of spars and ribs (Fig. 1). The main function of the wing spar webs and ribs is to resist the transverse shear force. Moreover, the multicellular arrangement looks like a sandwich honeycomb core. Hence, it is suitable to model them as the sandwich cores. To simplify the analysis and to get the overall effects, the multicellular arrangement of spar webs and ribs is modeled by using an equivalent shear modulus that should be related to the material properties and sizes of the wing spars and ribs. When uniform transverse shear strain is assumed over the wing cross section, the equivalent transverse shear modulus G_{yz} may be estimated by $G_{yz} = \tau_{yz}/\gamma_{yz}$, where τ_{yz} is the average transverse shear stress and may be calculated by dividing the total transverse shear force $\tilde{Q}_y$ over the wing cross section A_w, that is, $\tau_{yz} = \tilde{Q}_y/A_w$. The transverse shear strains can be calculated by

$$\gamma_{yz} = \frac{\tau_k}{G_k} = \frac{\tau_k A_k}{G_k A_k} = \frac{\sum \tau_k A_k}{\sum G_k A_k} = \frac{\tilde{Q}_y}{\sum G_k A_k}, \qquad k = 1, \ldots, n_s$$

where, τ_k, G_k, and A_k are the shear stress, shear modulus, and section area of the kth spar web and n_s is the number of the wing spars. By this calculation, the equivalent transverse shear modulus G_{yz} may be estimated as

$$G_{yz} = \sum_{k=1}^{n_s} G_k A_k \Big/ A_w \quad (16)$$

As for the transverse shear modulus G_{xz} that will be contributed by the wing ribs, no estimation is needed due to the assumption that $\gamma_{xz} = 0$. This also means that G_{xz} is assumed to be infinite under the construction of wing ribs. By Eq. (2b), the second equation in Eq. (5b), and Eqs. (10c), (10e), and (16), we now have

$$\tilde{Q}_y = \tilde{A}_{44}(\beta_f + w_f') + \tilde{A}_{44}^*(\beta_r - \theta') \quad (17)$$

Equilibrium Equations and Boundary Conditions

According to the postulation given in Eq. (10), the basic functions describing the deformation of the composite wing structures become v_0, w_f, θ, β_f, and β_r. The equilibrium equations corresponding to these basic functions will then be obtained by integrating Eq. (7) with respect to x. The associated integration and the results are

$$\int \left(\sum F_y = 0 \right) \mathrm{d}x : \frac{\mathrm{d}\tilde{N}_y}{\mathrm{d}y} + \tilde{p}_y = 0 \quad (18a)$$

$$\int \left(\sum F_z = 0 \right) \mathrm{d}x : \frac{\mathrm{d}\tilde{Q}_y}{\mathrm{d}y} + \tilde{p} = 0 \quad (18b)$$

$$\int \left[\left(\sum M_x = 0 \right) - x \left(\sum F_z = 0 \right) \right] \mathrm{d}x : \frac{d\left(\tilde{M}_{xy} - \tilde{Q}_y^*\right)}{\mathrm{d}y} + \tilde{m}_x - \tilde{p}^* = 0 \quad (18c)$$

$$\int \left(\sum M_y = 0 \right) \mathrm{d}x : \frac{\mathrm{d}\tilde{M}_y}{\mathrm{d}y} + \tilde{m}_y = \tilde{Q}_y \quad (18d)$$

$$\int \left(\sum M_y = 0 \right) x\,\mathrm{d}x : -\tilde{M}_{xy} + \frac{\mathrm{d}\tilde{M}_y^*}{\mathrm{d}y} + \tilde{m}_y^* = \tilde{Q}_y^* \quad (18e)$$

During the integration, the boundary values of N_{xy}, Q_x, M_x, and M_{xy} have been assumed to be zero for the present one-dimensional modeling [see Eq. (15) for the definition of tilde $\sim$ and superscript $*$]. $\tilde{N}_y$, $\tilde{Q}_y$, $\tilde{M}_y$, and $\tilde{M}_{xy}$ are related to the basic functions v_0, w_f, θ, β_f, and β_r by those given in Eqs. (14) and (17). By Eqs. (5a), (5b), and (11), $\tilde{Q}_y^*$ and $\tilde{M}_y^*$ may also be expressed in terms of the basic functions as

$$\tilde{Q}_y^* = \tilde{A}_{44}^*(\beta_f + w_f') + \tilde{A}_{44}^{**}(\beta_r - \theta') \quad (19a)$$

$$\tilde{M}_y^* = \tilde{B}_{22}^* v_0' + \tilde{D}_{22}^* \beta_f' + \tilde{D}_{22}^{**} \beta_r' + \tilde{D}_{26}^*(\theta' + \beta_r) \quad (19b)$$

The boundary conditions along $y = \text{const}$ can then be expressed as

$$\tilde{N}_y = \bar{\tilde{N}}_y, \quad \text{or} \quad v_0 = \bar{v}_0$$

$$\tilde{Q}_y = \bar{\tilde{Q}}_y, \quad \text{or} \quad w_f = \bar{w}_f$$

$$\tilde{M}_{xy} - \tilde{Q}_y^* = \bar{\tilde{M}}_{xy} - \bar{\tilde{Q}}_y^*, \quad \text{or} \quad \theta = \bar{\theta}$$

$$\tilde{M}_y = \bar{\tilde{M}}_y, \quad \text{or} \quad \beta_f = \bar{\beta}_f$$

$$\tilde{M}_y^* = \bar{\tilde{M}}_y^*, \quad \text{or} \quad \beta_r = \bar{\beta}_r \quad (20)$$

When the relations given in Eqs. (14), (17) and (19) are used, the equilibrium equations derived in Eq. (18) can be expressed in terms of five basic unknown functions v_0, w_f, θ, β_f, and β_r that constitute a 10th-order system of five ordinary differential equations. This system of equations can be completely solved with 10 boundary conditions described in Eq. (20), which consist of five boundary conditions for each edge.

Absence of Spanwise Loads

If the in-plane spanwise surface loads $\tilde{p}_y$ can be neglected, the 10th-order system of equations may be reduced to an equivalent 8th-order system of four ordinary differential equations in terms of four basic unknown functions w_f, θ, β_f, and β_r. With $\tilde{p}_y = 0$, the equilibrium equation in the y direction [Eq. (18a)] leads to $\tilde{N}_y = \text{const}$. If no in-plane spanwise loads are applied at the wingtip, this constant value will then be identical to zero. That is, $\tilde{N}_y = 0$ along the entire wing. When this result is substituted into the first Eq. (14), v_0' may be expressed in terms of β_f', β_r', and $\theta' + \beta_r$. Thus, the relations given in Eqs. (14) and (19b) can be simplified as

$$\begin{Bmatrix} \tilde{M}_y \\ \tilde{M}_{xy} \\ \tilde{M}_y^* \end{Bmatrix} = \begin{bmatrix} \breve{D}_{22} & \breve{D}_{22}^* & \breve{D}_{26} \\ \breve{D}_{26} & \breve{D}_{26}^* & \breve{D}_{66} \\ \breve{D}_{22}^* & \breve{D}_{22}^{**} & \breve{D}_{26}^* \end{bmatrix} \begin{Bmatrix} \beta_f' \\ \beta_r' \\ \theta' + \beta_r \end{Bmatrix} \tag{21}$$

where

$$\breve{D}_{ij} = \tilde{D}_{ij} - \tilde{B}_{i2}\tilde{B}_{2j}/\tilde{A}_{22}, \qquad \breve{D}_{ij}^* = \tilde{D}_{ij}^* - \tilde{B}_{i2}^*\tilde{B}_{2j}/\tilde{A}_{22}$$

$$\breve{D}_{ij}^{**} = \tilde{D}_{ij}^{**} - \tilde{B}_{i2}^*\tilde{B}_{2j}\big/\tilde{A}_{22}, \qquad i, j = 2, 6 \tag{22}$$

When the simplified relations derived in Eq. (21) are used together with Eqs. (17) and (19a), the remaining four equilibrium equations (18b–18e) then constitute an eighth-order system of four ordinary differential equations in terms of four basic unknown functions, w_f, θ, β_f, and β_r. Without considering the first condition of Eq. (20), the corresponding boundary conditions listed in Eq. (20) also reduce to four conditions for each edge.

Therefore, for a composite wing structure with the spanwise loads, as well as the distributed moments neglected, that is, $\tilde{p}_y = \tilde{N}_y = 0$ and $\tilde{m}_x = \tilde{m}_y = \tilde{m}_y^* = 0$, the equilibrium equations and boundary conditions given in Eqs. (18) and (20) can be reduced to

$$\frac{\mathrm{d}\tilde{Q}_y}{\mathrm{d}y} = -\tilde{p}, \qquad \frac{\mathrm{d}\left(\tilde{M}_{xy} - \tilde{Q}_y^*\right)}{\mathrm{d}y} = \tilde{p}^*$$

$$\frac{\mathrm{d}\tilde{M}_y}{\mathrm{d}y} = \tilde{Q}_y, \qquad -\tilde{M}_{xy} + \frac{\mathrm{d}\tilde{M}_y^*}{\mathrm{d}y} = \tilde{Q}_y^* \tag{23}$$

and at $y = 0$ (wing root)

$$w_f = \theta = \beta_f = \beta_r = 0 \tag{24a}$$

whereas at $y = l$ (wing tip)

$$\tilde{Q}_y = \tilde{M}_{xy} - \tilde{Q}_y^* = \tilde{M}_y = \tilde{M}_y^* = 0 \tag{24b}$$

Warping Restraint Effects

The importance of the warping restraint effects has been discussed in Refs. 7–10. Because of its importance, the warping restraint effects will not be neglected in this paper. This effect has been considered when we include β_r' in the expression of ε_y [second of Eqs. (3a)] in which κ_y is given in Eq. (11e). In other words, the free warping assumption can easily be done by letting $\beta_r' = 0$ in Eqs. (14), (19b), and all of the following related equations.

Governing Equations

To solve the problem established by the equilibrium equations (23) and the boundary conditions (24), we first express all of the functions in terms of four basic unknown functions, w_f, θ, β_f, and β_r. From Eqs. (17), (19a) and (21), the relations between $(\tilde{Q}_y, \tilde{M}_y, \tilde{M}_{xy}, \tilde{Q}_y^*, \tilde{M}_y^*)$ and $(w_f, \theta, \beta_f, \beta_r)$ can be written in matrix notation as

$$\boldsymbol{F} = \boldsymbol{K}_0\boldsymbol{\Delta} + \boldsymbol{K}_1\boldsymbol{\Delta}' \tag{25a}$$

where

$$\boldsymbol{F} = \begin{Bmatrix} \tilde{Q}_y \\ \tilde{M}_y \\ \tilde{M}_{xy} \\ \tilde{Q}_y^* \\ \tilde{M}_y^* \end{Bmatrix}, \qquad \boldsymbol{\Delta} = \begin{Bmatrix} w_f \\ \theta \\ \beta_f \\ \beta_r \end{Bmatrix}, \qquad \boldsymbol{K}_0 = \begin{bmatrix} 0 & 0 & \tilde{A}_{44} & \tilde{A}_{44}^* \\ 0 & 0 & 0 & \breve{D}_{26} \\ 0 & 0 & 0 & \breve{D}_{66} \\ 0 & 0 & \tilde{A}_{44}^* & \tilde{A}_{44}^{**} \\ 0 & 0 & 0 & \breve{D}_{26}^* \end{bmatrix}$$

$$\boldsymbol{K}_1 = \begin{bmatrix} \tilde{A}_{44} & -\tilde{A}_{44}^* & 0 & 0 \\ 0 & \breve{D}_{26} & \breve{D}_{22} & \breve{D}_{22}^* \\ 0 & \breve{D}_{66} & \breve{D}_{26} & \breve{D}_{26}^* \\ \tilde{A}_{44}^* & -\tilde{A}_{44}^{**} & 0 & 0 \\ 0 & \breve{D}_{26}^* & \breve{D}_{22}^* & \breve{D}_{22}^{**} \end{bmatrix} \tag{25b}$$

The system of equations (23) with boundary conditions given in Eqs. (24) can then be solved by using the technique of Laplace integral transform. This technique transforms Eq. (23) to a linear algebraic system of equations as

$$s\hat{\tilde{Q}}_y - \tilde{Q}_y(0) + \hat{\tilde{p}} = 0$$

$$s\left(\hat{\tilde{M}}_{xy} - \hat{\tilde{Q}}_y^*\right) - \tilde{M}_{xy}(0) + \tilde{Q}_y^*(0) - \hat{\tilde{p}}^* = 0$$

$$s\hat{\tilde{M}}_y - \tilde{M}_y(0) - \hat{\tilde{Q}}_y = 0, \qquad -\hat{\tilde{M}}_{xy} + s\hat{\tilde{M}}_y^* - \tilde{M}_y^*(0) - \hat{\tilde{Q}}_y^* = 0 \tag{26a}$$

or in matrix notation as

$$\boldsymbol{S}\hat{\boldsymbol{F}}(s) = \boldsymbol{J}\boldsymbol{F}(0) + \boldsymbol{P}(s) \tag{26b}$$

where

$$\boldsymbol{S} = \begin{bmatrix} s & 0 & 0 & 0 & 0 \\ 0 & 0 & s & -s & 0 \\ -1 & s & 0 & 0 & 0 \\ 0 & 0 & -1 & -1 & s \end{bmatrix}, \qquad \boldsymbol{J} = \begin{bmatrix} 1 & 0 & 0 & 0 & 0 \\ 0 & 0 & 1 & -1 & 0 \\ 0 & 1 & 0 & 0 & 0 \\ 0 & 0 & 0 & 0 & 1 \end{bmatrix}$$

$$\boldsymbol{P}(s) = \begin{Bmatrix} -\hat{\tilde{p}}(s) \\ \hat{\tilde{p}}^*(s) \\ 0 \\ 0 \end{Bmatrix} \tag{26c}$$

The caret $\hat{}$ denotes the Laplace transform, for example, $\hat{\tilde{Q}}_y(s) = L\{\tilde{Q}_y(y)\}$. By use of Eq. (25a), we have $\boldsymbol{F}(0) = \boldsymbol{K}_0\boldsymbol{\Delta}(0) + \boldsymbol{K}_1\boldsymbol{\Delta}'(0)$. The boundary condition (24a) means that $\boldsymbol{\Delta}(0) = \boldsymbol{0}$. Hence, $\boldsymbol{F}(0) = \boldsymbol{K}_1\boldsymbol{\Delta}'(0)$. The Laplace transform of Eq. (25a) plus the boundary condition $\boldsymbol{\Delta}(0) = \boldsymbol{0}$ leads to $\hat{\boldsymbol{F}}(s) = (\boldsymbol{K}_0 + s\boldsymbol{K}_1)\hat{\boldsymbol{\Delta}}(s)$. Substituting these results into Eq. (26b), we get the governing equations for the composite wing structures in the transformed domain of w_f, θ, β_f, and β_r, as

$$\boldsymbol{S}(\boldsymbol{K}_0 + s\boldsymbol{K}_1)\hat{\boldsymbol{\Delta}}(s) = \boldsymbol{J}\boldsymbol{K}_1\boldsymbol{\Delta}'(0) + \boldsymbol{P}(s) \tag{27}$$

and the boundary conditions remaining to be satisfied are those given in Eq. (24b). When the matrix notation and the relation given in Eq. (25a) are used, Eq. (24b) can be rewritten as

$$\boldsymbol{J}\boldsymbol{F}(l) = \boldsymbol{J}[\boldsymbol{K}_0\boldsymbol{\Delta}(l) + \boldsymbol{K}_1\boldsymbol{\Delta}'(l)] = \boldsymbol{0} \tag{28}$$

Aeroelastic Divergence

To study the aeroelastic divergence phenomena, the applied forces $\tilde{p}$ and $-\tilde{p}^*$ are considered as the lift and the aerodynamic nose-up

torsional moment (per unit length), respectively. In this paper, we will use the aerodynamic strip theory[18–20] to approximate the lift and the moment. In this approximation, one employs the known results for two-dimensional flow (infinite span airfoil) to calculate the aerodynamic forces on a lifting surface of finite span. Although this approximation may not be good for low aspect ratio wings, it is generally accepted for a preliminary study. By replacing the expressions for the lift and torsional moment with more accurate ones, and following the same steps described earlier, one may get updated results for the aeroelastic divergence problems. With this understanding, we now express $\tilde{p}(y)$ and $-\tilde{p}^*(y)$ for the static case considered as[5]

$$\tilde{p}(y) = aq_n c\theta_{\text{eff}}(y)$$

$$-\tilde{p}^*(y) = aq_n ce\theta_{\text{eff}}(y) + q_n c^2 C_{m,\text{ac}} \tag{29a}$$

where

$$\theta_{\text{eff}}(y) = \theta_0 + \theta(y) - w_f'(y)\tan\Lambda \tag{29b}$$

where a is the lift curve slope coefficient, q_n the dynamic pressure component normal to the leading edge, c the wing chord length, and e the distance between the lines of aerodynamic and flexural centers, both of which are considered to be constant in this paper. Also θ_0 is the angle of attack corresponding to the rigid-wing assumption, Λ the angle of sweep (positive for sweptback and negative for sweptforward), and $C_{m,\text{ac}}$ the pitching moment coefficient about the aerodynamic center, which will be constant with respect to the angle of attack. The related equations for q_n and a are

$$q_n = \frac{1}{2}\rho_0 V_n^2 = q\cos^2\Lambda, \qquad a = \frac{\mathrm{d}C_L}{\mathrm{d}\theta} = a_0\frac{\text{AR}}{\text{AR} + 4\cos\Lambda} \tag{29c}$$

where ρ_0 is the density of the airflow, V_n is the airflow velocity component normal to the leading edge, q is the dynamic pressure, C_L is the lift coefficient, a_0 is the corresponding two-dimensional lift-curve slope, AR is the wing aspect ratio defined as $\text{AR} \equiv (2l)^2/S = 2l/c$, where $2l$ is the wingspan measured as the distance between the two wingtips, and S ($=2cl$ in the case that c is independent of y) is the total area of the wing in the planform (x–y plane) view.

Taking the Laplace transform of Eq. (29a) and using the matrix notation defined in the third equation in Eq. (26c), we get

$$\boldsymbol{P}(s) = (1/s)\boldsymbol{P}_0 + \boldsymbol{\Gamma}\hat{\boldsymbol{\Delta}}(s) \tag{30a}$$

where

$$\boldsymbol{P}_0 = -q_n c\begin{Bmatrix} a\theta_0 \\ ae\theta_0 + cC_{m,\text{ac}} \\ 0 \\ 0 \end{Bmatrix}$$

$$\boldsymbol{\Gamma} = aq_n c\begin{bmatrix} s\tan\Lambda & -1 & 0 & 0 \\ se\tan\Lambda & -e & 0 & 0 \\ 0 & 0 & 0 & 0 \\ 0 & 0 & 0 & 0 \end{bmatrix} \tag{30b}$$

Substituting Eq. (30a) into Eq. (27), we get

$$\hat{\boldsymbol{\Delta}}(s) = \hat{\boldsymbol{K}}_s(s)[\boldsymbol{J}\boldsymbol{K}_1\boldsymbol{\Delta}'(0) + (1/s)\boldsymbol{P}_0] \tag{31a}$$

where

$$\hat{\boldsymbol{K}}_s(s) = [\boldsymbol{S}(\boldsymbol{K}_0 + s\boldsymbol{K}_1) - \boldsymbol{\Gamma}]^{-1} \tag{31b}$$

In Eq. (31b), $\hat{\boldsymbol{K}}_s(s)$ is a four by four matrix, and its inversion can be manipulated with the assist of symbolic computational software such as Mathematica or MATLAB®.[21] Implementing the inverse Laplace transform for Eq. (31a), we get

$$\boldsymbol{\Delta}(y) = \boldsymbol{K}_s(y)\boldsymbol{J}\boldsymbol{K}_1\boldsymbol{\Delta}'(0) + \left[\int_0^y \boldsymbol{K}_s(y)\,\mathrm{d}y\right]\boldsymbol{P}_0 \tag{32}$$

where $\boldsymbol{K}_s(y)$ is the inverse Laplace transform of $\hat{\boldsymbol{K}}_s(s)$. The unknown vector $\boldsymbol{\Delta}'(0)$ can then be determined by substituting Eq. (32) into the boundary condition (28), which leads to

$$\boldsymbol{J}[\boldsymbol{K}_0\boldsymbol{K}_s(l)\boldsymbol{J}\boldsymbol{K}_1 + \boldsymbol{K}_1\boldsymbol{K}_s'(l)\boldsymbol{J}\boldsymbol{K}_1]\boldsymbol{\Delta}'(0)$$
$$= -\boldsymbol{J}\left\{\boldsymbol{K}_0\left[\int_0^l \boldsymbol{K}_s(y)\,\mathrm{d}y\right] + \boldsymbol{K}_1\boldsymbol{K}_s(l)\right\}\boldsymbol{P}_0 \tag{33}$$

Equation (33) can address the problems of the static subcritical aeroelastic response and also that of the divergence instability. For the former problem, in the subcritical flight speed range, $\boldsymbol{\Delta}'(0)$ can be uniquely determined from the nonhomogeneous equation (33). The four basic functions $\boldsymbol{\Delta}(y) = (w_f, \theta, \beta_f, \beta_r)$ are then determined by Eq. (32). The resultant forces and bending moments $\boldsymbol{F}(y) = (\tilde{Q}_y, \tilde{M}_y, \tilde{M}_{xy}, \tilde{Q}_y^*, \tilde{M}_y^*)$ can also be found by the relation given in Eq. (25). On the other hand, when the flight speed reaches a certain value, the determinant of the coefficient matrix of $\boldsymbol{\Delta}'(0)$ in Eq. (33) may become zero, that is,

$$\|\boldsymbol{J}[\boldsymbol{K}_0\boldsymbol{K}_s(l)\boldsymbol{J}\boldsymbol{K}_1 + \boldsymbol{K}_1\boldsymbol{K}_s'(l)\boldsymbol{J}\boldsymbol{K}_1]\| = 0 \tag{34}$$

which will lead to the results that $\boldsymbol{\Delta}'(0)$ is infinite. In other words, under a certain condition the deflection of the wing structures may become infinite, which is the situation of aeroelastic divergence discussed in this paper. The lowest value of q for which the determinant vanishes corresponds to the critical (divergence) dynamic pressure q_d, and its associated velocity V_d is called divergence speed. The determination of divergence speed from the vanishing of the determinant shown in Eq. (34) can also be explained by the use of the eigenvalue concept. That is, for a homogeneous equation (33) (its right-hand side is taken to be zero), nontrivial solutions $\boldsymbol{\Delta}'(0)$ exist only when Eq. (34) is fulfilled. Under this condition, nonunique values of deflections exist, which is the condition of instability. The variation of the determinant with respect to the flow speed can be seen from the following relations: V_n is related to q_n through the first equation in Eq. (29c) and q_n will influence the determinant through $\boldsymbol{\Gamma}$ [Eq. (30b)], which in turn is related to $\hat{\boldsymbol{K}}_s(s)$ through Eq. (31b).

Numerical Results and Discussions

Knowing that the matrices $\boldsymbol{J}$ and $\boldsymbol{S}$ given in Eq. (26c) have nothing to do with the physical properties of the wing structures, from Eq. (34) and relation (31b) we see that the divergence speed will be influenced by $\boldsymbol{K}_0$, $\boldsymbol{K}_1$, and $\boldsymbol{\Gamma}$. By use of Eq. (25b), it is observed that $\boldsymbol{K}_0$ and $\boldsymbol{K}_1$ contain information of bending stiffness $\tilde{D}_{ij}$ and shearing stiffness $\tilde{A}_{44}$. From Eqs. (6), (12), (13), (15), and (22), we know that $\tilde{D}_{ij}$ will be influenced by the properties of the composite wing skin, stringers, spar flanges, and the shape of airfoil. From Eqs. (5b) and (16), we see that $\tilde{A}_{44}$ will be influenced by the properties of the spar webs and the shape of airfoil. The matrix $\boldsymbol{\Gamma}$ defined in Eq. (30b) contains information related to the aerodynamic characteristics such as c, e, a, Λ, and q_n defined in the paragraph between Eqs. (29) and (30). In the following examples, all of these factors will be studied numerically to see their influence on the divergence speed.

From Eq. (29b), it can be seen that the bending deformation tends to reduce the effective angle of attack for sweptback wings ($\Lambda > 0$), whereas in the case of sweptforward wings ($\Lambda < 0$), the opposite effect is valid. In other words, the bending deflections have a destabilizing effect on the sweptforward wings. That is why most of the recent studies devote their efforts to the aeroelastic tailoring of composite aircraft sweptforward wings. For this reason, most of the examples shown in this paper consider the sweptforward wings unless stated otherwise.

Because some special conditions of the present problems have been considered in the literature, before illustrating the general results we like to make some comparisons with the existing numerical solutions to verify our formulation.

Comparison with the Existing Numerical Solutions

Although the thickness of the wing structure is generally not very thin, most of the study on aeroelastic divergence problems did not consider the effect of transverse shear strain. Karpouzian and Librescu[10] included the transverse shear strain effect in their comprehensive model for an anisotropic composite aircraft wing and stated its importance on the aeroelastic divergence problems. However, only a flat rectangular isotropic wing model was used in their illustrating examples. Hence, the comparison can only be done on this special case. Moreover, the corresponding cases with the transverse shear strain neglected are also calculated to compare with other existing results.[4,7] The mechanical properties of the isotropic materials used for this comparison example are $E = 4.69$ GPa, $G = 1.88$ GPa, and $\nu = 0.25$. The plate thickness $h = 10$ cm. The wing chord length $c = 1$ m, and the aerodynamic data are $a_0 = 2\pi$ rad^{-1}, $C_{m,\mathrm{ac}} = 0.0$, $e/c = 0.1$, and $\theta_0 = 5$ deg. The results with the transverse shear strain neglected are shown in Fig. 4 for the divergence dynamic pressure vs aspect ratio, whereas those considering the effect of transverse shear strain are presented in Table 1 for the subcritical static aeroelastic response. Both Fig. 4 and Table 1 show that our results agree well with the existing numerical solutions. The results presented in Table 1 also show that the values of $[\theta_{\mathrm{eff}}/\theta_0]_{y=l}$ corresponding to the nonshearable wing model, that is, $E/G_{yz} = 0$, underestimate the static response by a large amount as compared to the shearable wing model, as represented by $E/G_{yz} = 40$, 60, and 100 considered in this paper.

Table 1 Subcritical static aeroelastic response for uniform isotropic swept-wing model with transverse shear strain included

Case	E/G_{yz}	$[\theta_{\mathrm{eff}}/\theta_0]_{y=l}$ Karpouzian and Librescu[10]	$[\theta_{\mathrm{eff}}/\theta_0]_{y=l}$ Present solution
AR = 6, Λ = −20 deg	0	4.45	4.35
q = 52,401 Pa (WR)[a]	60	5.35	5.23
	100	6.05	5.98
AR = 6, Λ = −40 deg	0	8.6	8.53
q = 39,440 Pa (WR)	60	10.9	10.82
AR = 8, Λ = −60 deg	40	5.3	5.42
q = 14,811 Pa (WR)			
AR = 6, Λ = −40 deg	60	11.4	11.37
q = 39,440 Pa (FR)[b]			

[a] Warping restraint (WR) effect is considered.
[b] Free warping (FW) condition is assumed.

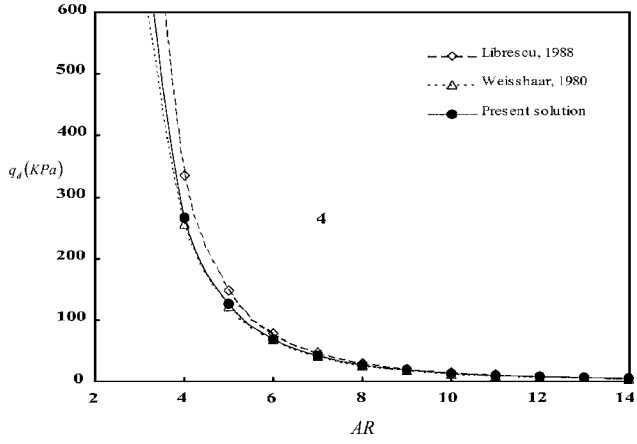

Fig. 4 Divergence dynamic pressure vs aspect ratio for uniform isotropic swept-wing model with transverse shear strain neglected, Λ = − 20 deg.

After verifying our results by using the flat rectangular isotropic wing model, in the following numerical illustrations we will consider a composite wing structure with the NACA 2412 airfoil. From the data given in Table 2 (Ref. 22) (with the origin located at the midchord line), this airfoil is simulated by a ninth-order polynomial. Its associated aerodynamic data are $a_0 = 5.73$ rad^{-1}, $C_{m,\mathrm{ac}} = -0.04$, $e/c = 0.257$, and $\theta_0 = 5$ deg. The wing chordwise length $c = 1$ m. The wing skin is made of graphite/epoxy fiber-reinforced composite whose mechanical properties are $E_{11} = 200$ GPa, $E_{22} = 5$ GPa, $\nu_{12} = 0.25$, $G_{12} = 2.5$ GPa, and ply thickness $t = 0.25$ mm. Three different arrangements for the composite wing skin will be considered: 1) [90/−45/45/0] for upper skin and [0/45/−45/90] for lower skin, 2) [90/45/−45/0] for upper skin and [0/−45/45/90] for lower skin, and 3) $[\phi_f)_{20}]$ for upper and lower skins. Two wing spars made of isotropic materials with shear modulus $G = 8$ GPa and thickness 6 mm are located at $\pm 0.25c$ from the midchord line in most of the examples unless stated otherwise (Fig. 5).

Table 2 NACA 2412 airfoil[22]

x/c	$(1/c)f_u(x/c)$	$(1/c)f_l(x/c)$
−0.5	0.0	0.0
−0.4875	0.0215	−0.0165
−0.475	0.0299	−0.0227
−0.45	0.0413	−0.0301
−0.425	0.0496	−0.0346
−0.4	0.0563	−0.0375
−0.35	0.0661	−0.041
−0.3	0.0726	−0.0423
−0.25	0.0767	−0.0422
−0.2	0.0788	−0.0412
−0.1	0.078	−0.038
0	0.0724	−0.0334
0.1	0.0636	−0.0276
0.2	0.0518	−0.0214
0.3	0.0375	−0.015
0.4	0.0208	−0.0082
0.45	0.0114	−0.0048
0.5	0.0	−0.0

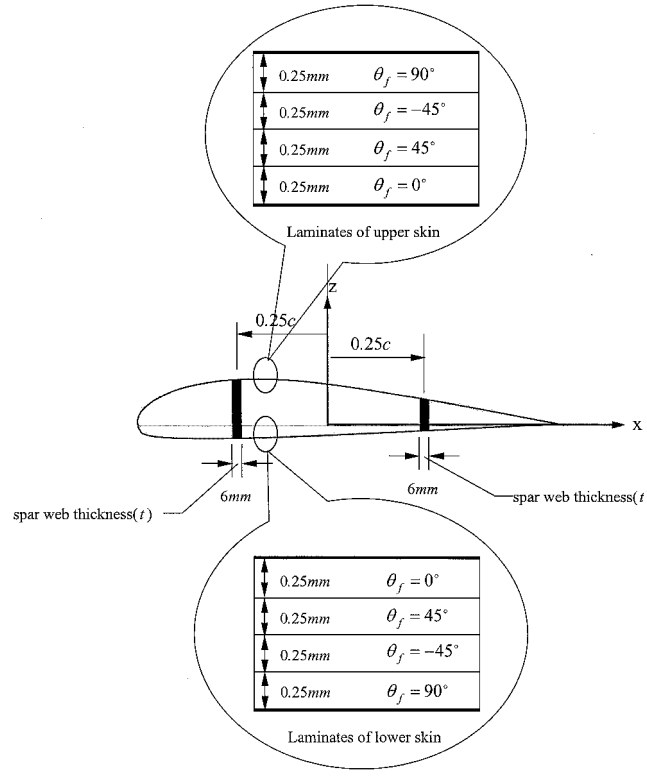

Fig. 5 Example of composite multicell wing structures.

Table 3 The effects of transverse shear deformation on the slope of bending deflection and the angle of attack, AR = 8

Span position y/l	θ_{eff}		θ		w'_f	
	w/o TS[a]	w/TS[b]	w/o TS[a]	w/TS[b]	w/o TS[a]	w/TS[b]
			$q = 12,420$ Pa, $\Lambda = -30$ deg			
0.2	1.96×10^{-1}	2.14×10^{-1}	4.87×10^{-3}	9.21×10^{-3}	1.79×10^{-1}	2.03×10^{-1}
0.6	3.05×10^{-1}	3.39×10^{-1}	1.46×10^{-2}	2.46×10^{-2}	3.52×10^{-1}	3.93×10^{-1}
1.0	3.24×10^{-1}	3.59×10^{-1}	1.92×10^{-2}	3.02×10^{-2}	3.77×10^{-1}	4.19×10^{-1}
			$q = 12{,}420$ Pa, $\Lambda = 30$ deg			
0.2	6.88×10^{-2}	6.87×10^{-2}	-3.83×10^{-4}	-2.85×10^{-5}	3.13×10^{-2}	3.21×10^{-2}
0.6	5.21×10^{-2}	5.24×10^{-2}	-1.19×10^{-3}	-4.79×10^{-4}	5.89×10^{-2}	5.96×10^{-2}
1.0	4.94×10^{-2}	5.01×10^{-2}	-1.63×10^{-3}	-6.67×10^{-4}	6.28×10^{-2}	6.32×10^{-2}
			$q = 4{,}140$ Pa, $\Lambda = -60$ deg			
0.2	1.03×10^{-1}	1.03×10^{-1}	1.52×10^{-4}	3.02×10^{-4}	8.83×10^{-3}	9.04×10^{-3}
0.6	1.17×10^{-1}	1.18×10^{-1}	4.44×10^{-4}	7.60×10^{-4}	1.71×10^{-2}	1.73×10^{-2}
1.0	1.19×10^{-1}	1.20×10^{-1}	5.50×10^{-4}	9.22×10^{-4}	1.83×10^{-2}	1.84×10^{-2}
			$q = 4{,}140$ Pa, $\Lambda = 60$ deg			
0.2	7.81×10^{-2}	7.80×10^{-2}	2.64×10^{-5}	1.04×10^{-4}	5.30×10^{-3}	5.41×10^{-3}
0.6	6.98×10^{-2}	6.99×10^{-2}	6.63×10^{-5}	2.24×10^{-4}	1.01×10^{-2}	1.02×10^{-2}
1.0	6.86×10^{-2}	6.88×10^{-2}	7.83×10^{-5}	2.63×10^{-4}	1.08×10^{-2}	1.08×10^{-2}

[a] $G_{yz} = \infty$ with transverse shear deformation neglected (w/o TS). [b] $G_{yz} = 84$ MPa with transverse shear effect included (w/TS).

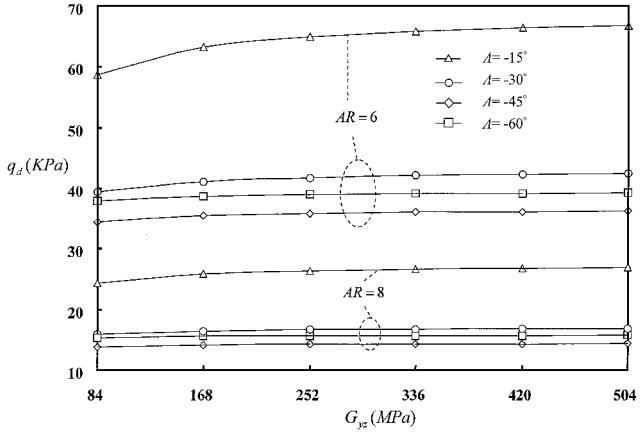

Fig. 6 Effects of equivalent transverse shear modulus on the divergence dynamic pressure.

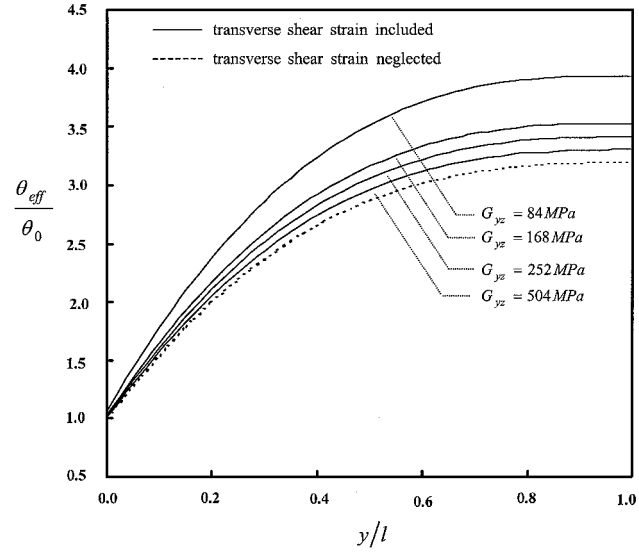

Fig. 7 Effects of equivalent transverse shear modulus on the distribution of the angle of attack, AR = 6, Λ = − 30 deg, and q = 30 kPa.

Effects of Spar Webs

Through the modeling given in Eq. (16), we know that consideration of the spar web effects is equivalent to the transverse shear strain effects. The importance of the transverse shear strain effects has been revealed by the numerical illustration provided in the work of Karpouzian and Librescu[10] for the case of uniform rectangular isotropic wing. In this paper, the composite wing with arrangement 1 given earlier is considered. Figure 6 shows the effects of equivalent transverse shear modulus on the divergence dynamic pressure. From this result we see that the larger the transverse shear modulus is the higher the divergence dynamic pressure, which is reasonable and to be expected. Moreover, this effect is more pronounced when the sweptforward angle is smaller and/or the aspect ratio is smaller. Consider AR = 6, $\Lambda = -30$ deg, and $q = 30$ kPa, Fig. 7 shows the effects of equivalent transverse shear modulus on the angle of attack, from which we see that the larger the transverse shear modulus is the closer to the cases that the transverse shear strains are neglected. This is also reasonable because the neglect of the transverse shear strain means that its corresponding modulus is assumed to be infinite. Similar results can also be obtained for the other aspect ratios, sweptforward angles, and dynamic pressure.[23]

Table 3 shows that transverse shear deformability yields an increase of the slope of bending deflection w'_f and, as a result [observed from Eq. (29b)], exacerbates not only the wash-in effect for sweptforward wings ($\Lambda < 0$) but also the wash-out effect for sweptback wings ($\Lambda > 0$). This interesting effect was also observed in the case of aircraft wings modeled as thin-walled beams.[24] The effective angle of attack θ_{eff} for the sweptforward wings increases due to the increases of θ and w'_f if the effect of transverse shear deformation is considered. However, for the sweptback wings, the effective angle of attack may not decrease even w'_f increases with transverse shear deformability included because θ may not necessarily decrease.

Effects of Skin Stiffness

To study the effects of skin stiffness, we may vary the mechanical properties of the composite, the fiber orientation, or the ply stacking sequence. With aspect ratio AR = 6, Fig. 8 shows the results for arrangement 3 of unidirectional composite skin. From Fig. 8, we see that there is a range, for example, $90 \le \phi_f \le 130$ deg for $\Lambda = -30$ deg, where the divergence dynamic pressure is very large and cannot be shown. This also means that when the fiber is oriented in this range there will be no divergence problems. Moreover, the stability range is narrower for larger sweptforward angles. These phenomena are similar to those discussed by Weisshaar[4] for the case of flat wings without considering the transverse shear deformation.

For the effects of ply stacking sequence, a series of numerical results[23] are obtained for the arrangements 1 and 2 (the plies of ±45 deg have been increased three times to magnify the effects of

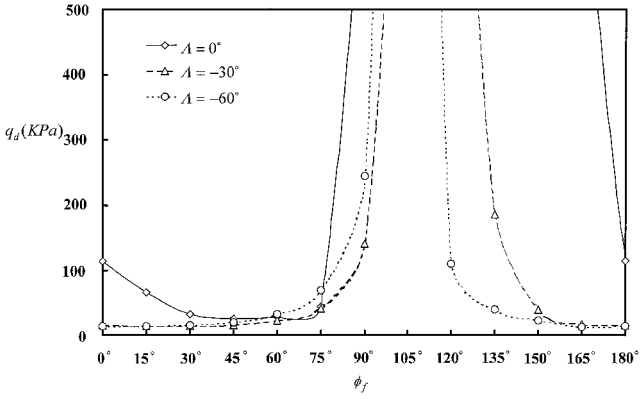

Fig. 8 Effects of fiber orientation on the divergence dynamic pressure.

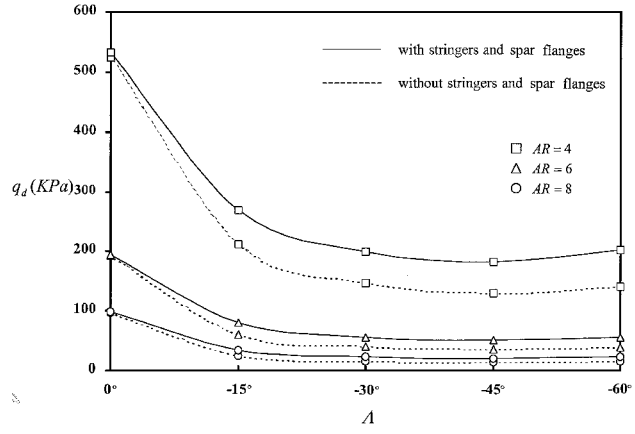

Fig. 9 Effects of stringers and spar flanges on the divergence dynamic pressure.

stacking sequence). All of these results show that the divergence dynamic pressure of arrangement 1 is larger than that of arrangement 2, which is consistent with the results for the effects of fiber orientation. That is, the fiber orientation $\phi_f = -45$ deg (or, for example, $\phi_f = 135$ deg) is better than $\phi_f = 45$ deg for the consideration of aeroelastic divergence. The arrangement of better orientation on the outer part of the laminates will provide better bending stiffness. Therefore, arrangement 1 with $\phi_f = -45$ deg located on the outer ply will be better than arrangement 2 with $\phi_f = -45$ deg located on the inner ply.

In addition to the cases of composite laminates, several other kinds of materials such as aluminium and titanium are also used to study the effects of skin stiffness.[23] All of these results show that the larger the stiffness is, the higher the divergence dynamic pressure, which is reasonable and to be expected.

Effects of Stringers and Spar Flanges

From the modeling given in Eq. (12), we know that the main contribution of the stringers and spar flanges is resisting the bending and axial loads, which should reasonably increase the ability of resisting the aeroelastic divergence. Hence, our curiosity turns to how much will they increase the divergence dynamic pressure. Figure 9 shows the divergence dynamic pressure with or without the stringers (including the spar flanges) will have some discrepancy, such as 26.9% difference ($q_d = 212$ kPa without stringers and $q_d = 269$ kPa with stringers) for AR = 4, $\Lambda = -15$ deg, and 48.7% difference ($q_d = 15.4$ kPa without stringers and $q_d = 22.9$ kPa with stringers) for AR = 8, $\Lambda = -60$ deg. Here, composite arrangement 1 is used, and $E_s = E_f = 69$ GPa, $v_s = v_f = 0.33$, $A_s = 7$ cm^2, $A_f = 1.4$ cm^2, and $A_p = 150$ cm^2. Without stringers and spar flanges, the bending stiffness $D_{22} = 326$ kPa $\cdot$ m^4, whereas $D_{22} = 497$ kPa $\cdot$ m^4 with stringers and spar flanges included. That is, with the inclusion of stringers and spar flanges, the bending stiffness in y direction is increased by 52%, and its associated increase in the divergence dynamic pressure is generally lower than 52%. From Fig. 8, we see that the lowest difference (about 1%) occurs in the case of $\Lambda = 0$ deg.

Effects of Swept Angle, Aspect Ratio, and Shape of Airfoil

It is well known that bending deflections have a destabilizing/stabilizing effect on the sweptforward/back wings and, hence, the divergence speed will be decreased/increased. It is also known that the larger the aspect ratio is the more flexible the wing and, hence, the lower the divergence speed. All of the related numerical examples for the composite wings discussed in this paper show this tendency.[20] To save space, we will not list these results. For the approximation of airfoil shape, Fig. 10 and Table 4 show that 4.7% error of approximation will lead to 35% error of divergence speed. If the error of approximation is restricted to within 0.4%, the corresponding error for the divergence speed will be under 1% (Ref. 23).

Warping Restraint Effects

The warping restraint effects have been discussed in Refs. 7–10. Similar work has also been done for the present composite wing model, as shown in Fig. 11. In addition to this, most of the results shown in the work of Tsai[23] reveal that consideration of the warping restraint effects will increase the divergence dynamic pressure, although some of them may lower the divergence dynamic pressure, which is consistent with the conclusion given in Refs. 7–10.

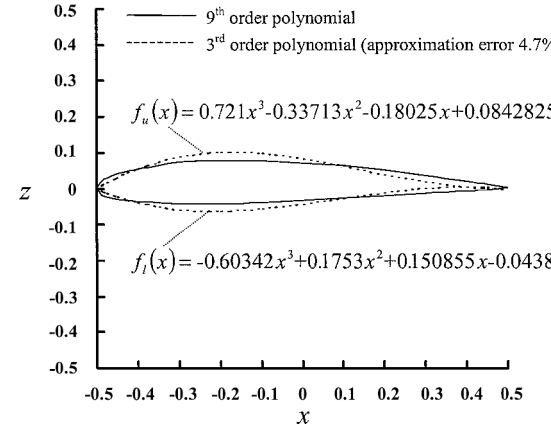

Fig. 10 Effects of airfoil shape on the divergence dynamic pressure, NACA 2412, c = 1 m.

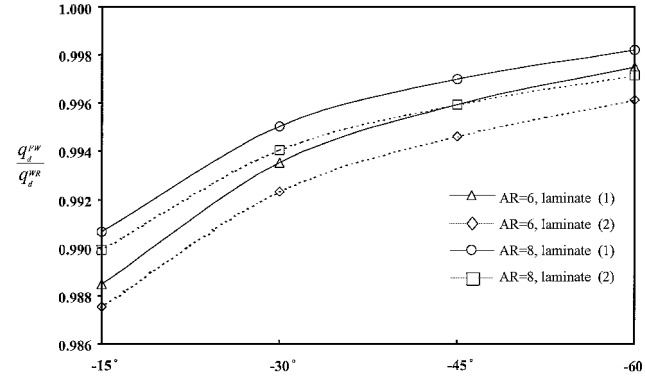

Fig. 11 Effects of warping restraint on the divergence dynamic pressure, q_d^{FW} divergence dynamic pressure of free warping model, q_d^{WR} divergence dynamic pressure with warping restraint effects included; laminate 1, [90/$-$ 45$_3$/45$_3$/0] for upper skin and [0/45$_3$/$-$ 45$_3$/90] for lower skin, and laminate 2, [90/45$_3$/$-$ 45$_3$/0] for upper skin and [0/$-$ 45$_3$/45$_3$/90] for lower skin.

Table 4 Effects of airfoil shape on divergence dynamic pressure

Λ, deg	Ninth-order polynomial	Third-order polynomial	Error, %
	$AR = 6$, q_d Pa		
−15	60,526	81,617	34.85
−30	40,073	54,134	35.10
−45	34,881	47,161	35.21
−60	38,214	51,695	35.28
	$AR = 8$, q_d Pa		
−15	24,972	33,762	35.20
−30	16,074	21,752	35.32
−45	13,937	18,870	35.40
−60	15,397	20,851	35.42

Conclusions

By direct integration with respect to x for the equilibrium equations and boundary conditions of the composite sandwich plates, explicit and relatively simple mathematical expressions for the aeroelastic divergence of stiffened composite multicell wing structures have been derived. In the present model, several factors are considered in one unified formulation such as the effects of composite skins, spars, stringers, swept angles, aspect ratio, shape of airfoil, and warping restraints. In the literature, because of the mathematical complexity, most of the effects are treated separately. Moreover, their final expressions are usually symbolic and not explicitly written. In addition, in the present model we provide a very simple way to model the stringers, spars, and ribs of multicell wing structures. Although this modeling, such as Eqs. (12) and (16), looks simple and familiar, to the authors' knowledge it has not been raised previously. Perhaps because of the lack of this simple modeling and the complexity of the inclusion of airfoil shapes, in the literature no examples of multicell wing structures with airfoil shapes have been discussed for the aeroelastic divergence problems. To show that our model is simple, general, and correct, several examples including all of these factors are presented.

A comparison example for flat rectangular isotropic wings has been done, and our results agree well with the existing numerical solutions. In addition, to show the generality of our solutions, a composite wing with NACA 2412 airfoil is illustrated. The effects of spars, skins (including the ply orientation and stacking sequence), stringers, swept angles, aspect ratio, shape of airfoil, and the warping restraints on the divergence dynamic pressures and the lift loads redistribution are all studied. The results show that these effects preserve the same trend as those of the flat composite wing structure assumptions except that their values will be influenced by the shape of airfoil. Moreover, the addition of stringers and spars will increase the divergence dynamic pressure and lower the effective angle of attack by an amount lower than the stiffness increment.

Acknowledgments

The authors would like to thank the support by National Science Council through Grant NSC 82-0401-E006-356and NSC 89-2212-E-006-192.

References

[1]Diederich, F. W., and Budiansky, B., "Divergence of Swept Wings," NASA TN 1680, Aug. 1948.

[2]Krone, N. J., Jr., "Divergence Elimination with Advanced Composites," AIAA Paper 75-1009, Aug. 1975.

[3]Lerner, E., and Markowitz, J., "An Efficient Structural Resizing Procedure for Meeting Static Aeroelastic Design Objectives," *Journal of Aircraft*, Vol. 16, No. 2, 1979, pp. 65–71.

[4]Weisshaar, T. A., "Divergence of Forward Swept Composite Wings," *Journal of Aircraft*, Vol. 17, No. 6, 1980, pp. 442–448.

[5]Oyibo, G. A., "Generic Approach to Determine Optimum Aeroelastic Characteristics for Composite Forward-Swept-Wing Aircraft," *AIAA Journal*, Vol. 22, No. 1, 1984, pp. 117–123.

[6]Lottati, I., "Flutter and Divergence Aeroelastic Characteristics for Composite Forward Swept Cantilevered Wing," *Journal of Aircraft*, Vol. 22, No. 11, 1985, pp. 1001–1007.

[7]Librescu, L., and Simovich, J., "General Formulation for the Aeroelastic Divergence of Composite Swept-Forward Wing Structures," *Journal of Aircraft*, Vol. 25, No. 4, 1988, pp. 364–371.

[8]Librescu, L., and Khdeir, A. A., "Aeroelastic Divergence of Swept-Forward Composite Wings Including Warping Restraint Effect," *AIAA Journal*, Vol. 26, No. 11, 1988, pp. 1373–1377.

[9]Librescu, L., and Thangjitham, S., "Analytical Studies on Static Aeroelastic Behavior of Forward-Swept Composite Wing Structures," *Journal of Aircraft*, Vol. 28, No. 2, 1991, pp. 151–157.

[10]Karpouzian, G., and Librescu, L., "Comprehensive Model of Anisotropic Composite Aircraft Wings Suitable for Aeroelastic Analyses," *Journal of Aircraft*, Vol. 31, No. 3, 1994, pp. 703–712.

[11]Hwu, C., and Hu, J. S., "Buckling and Postbuckling of Delaminated Composite Sandwich Beams," *AIAA Journal*, Vol. 30, No. 7, 1992, pp. 1901–1909.

[12]Hu, J. S., and Hwu, C., "Free Vibration of Delaminated Composite Sandwich Beams," *AIAA Journal*, Vol. 33, No. 9, 1995, pp. 1–8.

[13]Kirchhoff, G., *Vorlesungen über mathematische Physik*, Vol. 1, B. G. Teubner, Leipzig, Germany, 1876.

[14]Reissner, E., "The Effect of Transverse Shear Deformation on the Bending of Elastic Plates," *Journal of Applied Mechanics*, Vol. 12, No. 2, 1945, pp. A69–A77.

[15]Jones, R. M., *Mechanics of Composite Materials*, Scripta, Washington, DC, 1975, Chap. 4, pp. 147–237.

[16]Cowper, G. R., "The Shear Coefficient in Timoshenko's Beam Theory," *Journal of Applied Mechanics*, Vol. 3, No. 2, 1966, pp. 335–340.

[17]Megson, T. H. G., *Aircraft Structures—for Engineering Students*, 2nd ed. Edward Arnold, London, 1990, Chap. 8, pp. 225–311.

[18]Fung, Y. C., *An Introduction to the Theory of Aeroelasticity*, Wiley, New York, 1955, Chap. 3, pp. 81–112.

[19]Bisplinghoff, R. L., Asheley, H., and Halfman, R. L., *Aeroelasticity*, Addison–Wesley, Cambridge, MA, 1955, Chap. 8, pp. 421–526.

[20]Dowell, E. H., Curtiss, H. C., Jr., Scanlan, R. H., and Sisto, F., *A Modern Course in Aeroelasticity*, Sijthoff and Noordhoff, Alphen aan den Rijn, The Netherlands, 1978, Chap. 2, pp. 3–46.

[21]Hanselman, D., and Littlefield, B., *The Student Edition of MATLAB*, Prentice–Hall, Englewood Cliffs, NJ, 1995.

[22]Hunsaker, J. C., *Theory of Wing Sections*, McGraw–Hill, New York, 1949, p. 410.

[23]Tsai, Z. S., "Aeroelastic Divergence of Composite Wing Structures," M.S. Thesis, Inst. of Aeronautics and Astronautics, National Cheng-Kung Univ., Tainan, Taiwan, Republic of China, June 2000.

[24]Librescu, L., and Song, O., "On the Static Aeroelastic Tailoring of Composite Aircraft Swept Wings Modelled as Thin-Walled Beams Structures," *Composite Engineering*, Special issue: Use of Composite in Rotor Craft and Smart Structures, Vol. 2, No. 5–7, 1992, pp. 497–512.